Atomic layer deposition of (K,Na)(Nb,Ta)O_3 thin films

Henrik Hovde Sønsteby, Ola Nilsen, and Helmer Fjellvåg

Citation: Journal of Vacuum Science & Technology A: Vacuum, Surfaces, and Films **34**, 041508 (2016); doi: 10.1116/1.4953406

View online: http://dx.doi.org/10.1116/1.4953406

View Table of Contents: http://avs.scitation.org/toc/jva/34/4

Published by the American Vacuum Society

Articles you may be interested in

Crystallinity of inorganic films grown by atomic layer deposition: Overview and general trends
Journal of Vacuum Science & Technology A: Vacuum, Surfaces, and Films **113**, 021301021301 (2013); 10.1063/1.4757907

Instruments for Advanced Science

Contact Hiden Analytical for further details:
W www.HidenAnalytical.com
E info@hiden.co.uk
CLICK TO VIEW our product catalogue

Gas Analysis
- dynamic measurement of reaction gas streams
- catalysis and thermal analysis
- molecular beam studies
- dissolved species probes
- fermentation, environmental and ecological studies

Surface Science
- UHV TPD
- SIMS
- end point detection in ion beam etch
- elemental imaging - surface mapping

Plasma Diagnostics
- plasma source characterization
- etch and deposition process reaction
- kinetic studies
- analysis of neutral and radical species

Vacuum Analysis
- partial pressure measurement and control of process gases
- reactive sputter process control
- vacuum diagnostics
- vacuum coating process monitoring

Atomic layer deposition of (K,Na)(Nb,Ta)O_3 thin films

Henrik Hovde Sønsteby,[a] Ola Nilsen, and Helmer Fjellvåg
Department of Chemistry, University of Oslo, Sem Sælands vei 26, 0371 Oslo, Norway

(Received 1 March 2016; accepted 23 May 2016; published 8 June 2016)

Thin films of complex alkali oxides are frequently investigated due to the large range of electric effects that are found in this class of materials. Their piezo- and ferroelectric properties also place them as sustainable lead free alternatives in optoelectronic devices. Fully gas-based routes for deposition of such compounds are required for integration into microelectronic devices that need conformal thin films with high control of thickness- and composition. The authors here present a route for deposition of materials in the (K,Na)(Nb,Ta)O_3-system, including the four end members $NaNbO_3$, $KNbO_3$, $NaTaO_3$, and $KTaO_3$, using atomic layer deposition with emphasis on control of stoichiometry in such mixed quaternary and quinary compunds. © *2016 American Vacuum Society*.
[http://dx.doi.org/10.1116/1.4953406]

I. INTRODUCTION

Thin films of $A^IB^VO_3$ perovskites based on alkaline A^I elements obtain an increasing amount of attention due to the many important physical properties that are found in materials of this class. $LiNbO_3$ and $K_xNa_{1-x}NbO_3$ are both considered strong candidates as sustainable lead free piezo- and ferroelectrics in many applications.[1–5] $LiTaO_3$ is renowned for its piezoelectric properties.[6] Anion doped $NaTaO_3$ is used in visible light photocatalysis.[7] $KNbO_3$ is already in use in devices utilizing surface acoustic waves and in nonlinear optics.[8,9] $KTaO_3$ is under investigation for forming a 2D electron gas at interfaces toward $LaTiO_3$ analogous to the $SrTiO_3$||$LaAlO_3$ heteroepitaxial system.[10] In addition to this, multilayer stacks of $KTaO_3$||$KNbO_3$ are reported to exhibit a strong ferroelectric response.[11]

Thin films of several $A^IB^VO_3$-materials have been deposited using physical deposition techniques such as pulsed laser deposition, molecular beam epitaxy and sputtering;[12–21] however, reports on low temperature chemical deposition routes are very limited. Thin films of $LiNbO_3$, $LiTaO_3$, and $KNbO_3$ have been grown using chemical vapor deposition,[22–24] and $LiNbO_3$ and $LiTaO_3$ is also reported by atomic layer deposition (ALD).[25,26] ALD would indeed be the technique of choice in many the potential applications due to excellent thickness control and conformality of the deposited films, in particular, on very high aspect ratio substrates.[27] These are crucial features in applications utilizing surface acoustic waves and in optoelectronics. However, the lack of suitable precursors has so far limited the possibility of ALD-grown sodium- and potassium containing thin films. In 2014, ALD of sodium- and potassium aluminates were reported for the first time, thereby opening for growth of a range of materials containing these elements.[28]

In this work, ALD of the four-component (K,Na)(Nb,Ta)O_3-system is investigated. In addition to this, evidence of complete intermixing of all the four end members is provided.

[a]Electronic mail: henrik.sonsteby@kjemi.iuio.no

II. EXPERIMENT

All thin films in this work were deposited using a Beneq TFS-500 atomic layer deposition reactor. The depositions were carried out at 3 mbar working pressure, with N_2 as the carrier- and purging gas. Nitrogen gas was supplied from a Schmidelin-Sirrco 5 generator providing >99.9995% (N_2 + Ar) before purification through a Mykrolis purifier. Reactor temperature was maintained at 250 °C unless otherwise stated, consistent with previous reports of ALD-growth of similar compounds.

Sodium- and potassium *tert*-butoxide were used as alkali metal sources, supplied from HS-300 sources at 140 and 150 °C, respectively. Niobium- and tantalum ethoxide was used as group V metal sources, supplied from a HS-500 source at 68 and 70 °C, respectively. The precursors were supplied through heated valves. The metalorganic precursors used are summarized in Table I. Distilled water was used as the oxygen source. The water pulse was set to 0.25 s, and the purge duration to 1 s for all experiments. The *tert*-butoxides were pulsed for 3 s whereas the ethoxides were pulsed for 2 s. All pulse and purge parameters are well within self-limiting growth as shown by earlier experiments.[28–30]

All systems were developed by depositing on Si(100) $1 \times 1\,cm^2$ single crystal substrates. A Pt-coated Si(100) substrate was used for piezoelectric characterization of one $K_{0.5}Na_{0.5}NbO_3$ thin film.

Thin film thickness was measured using a J. A. Woolam α-SE spectroscopic ellipsometer in the range of 390–900 nm. A Cauchy-function was used to model the data assuming the films were transparent in this wavelength range.

Cation compositions of the films were measured with standardless x-ray fluorescence spectroscopy using a Philips

TABLE I. Overview of the precursors used.

Chemical name	Formula	Supplier	Purity
Sodium *tert*-butoxide	$NaOC(CH_3)_3$	Aldrich	97%
Potassium *tert*-butoxide	$KOC(CH_3)_3$	Aldrich	98%
Niobium ethoxide	$Nb(OCH_2CH_3)_5$	Aldrich	99.9%
Tantalum ethoxide	$Ta(OCH_2CH_3)_5$	Aldrich	99.9%

 © 2016 American Vacuum Society

PW2400 XRF and analyzed using the UNIQUANT software package.

Complementary measurements of composition using x-ray photoelectron spectroscopy were performed using a Thermo Scientific Theta Probe Angle-Resolved XPS system, also enabling measurements of carbon contaminants and possible segregation of the cations in the films. The instrument is equipped with a standard Al Kα source ($h\nu = 1486.6$ eV), and the analysis chamber pressure is in the order of 10^{-8} mbar. Pass energy values of 200 and 50 eV were used for survey spectra and detailed scans, respectively.

Crystallographic studies were performed on a PANalytical Empyrean diffractometer equipped with a Cu Kα ($\lambda = 1.5406$ Å) source powered at 45 kV and 40 mA. A parallel beam x-ray mirror and a proportional point detector were used for grazing incidence x-ray diffraction (GIXRD) measurements.

Morphology studies were performed using a Park Systems XE-70 AFM equipped with a standard non-contact high-resolution tip. Data were analyzed using the Gwyddion 2.43 SPM visualization tool.[31] The same apparatus equipped with an enhanced piezoresponse force microscopy (PFM) tip and lock-in amplifier was used for mapping of piezoelectric domains in a $K_{0.5}Na_{0.5}NbO_3$ thin film.[32] PFM works by applying an AC current through a conductive AFM tip to achieve piezoelectric deformation of the sample, thereby directly measuring the piezoelectric domains.

III. RESULTS AND DICSUSSION

A. Thin film growth

The thin films were in general grown as a mix of two, three, or four well known processes for binary systems: K-O, Na-O, Nb-O, and Ta-O. In all these processes, water is used as the oxygen source, keeping the amount of precursors to a minimum and ruling out issues with stronger oxidizing agents such as O_3 that may interfere with layer-by-layer growth of the alkali metal precursors. This effect was seen for the alkali aluminate systems, where the ozone based process resulted in higher carbon contamination due to formation of carbonates.[28] Tantalum oxide and niobium oxide were deposited with a growth rate of 0.40 ± 0.01 and 0.38 ± 0.01 Å/cycle, respectively, close to previously reported values by Kukli *et al.*[29,30] It is not possible to examine the alkali metal binary systems as pure oxides due to the formation of hydroxides or carbonates. They were therefore initially deposited as aluminates as described by Østreng *et al.* to verify similar growth rates.[28] All precursors exhibit self-limiting reactions with traditional ALD type growth for the pulse parameters applied (also see the supplementary material).[33]

The four end $A^{I}B^{V}O_3$-members in the (K,Na)(Nb,Ta)O_3-system were deposited by combining two binary systems to create a ternary reaction cycle. The *net* super cycle for all four compounds can be described as

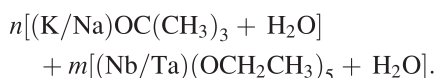

$$n[(K/Na)OC(CH_3)_3 + H_2O] + m[(Nb/Ta)(OCH_2CH_3)_5 + H_2O].$$

The pulsing sequence was chosen as to facilitate maximum mixing, i.e., a pulsed net 2:3 ratio was deposited as (K/Na) + (Nb/Ta) + (K/Na) + (Nb/Ta) + (Nb/Ta). All four end member systems showed typical ALD-behavior, and conformal thin films were obtained. The required n and m values for obtaining stoichiometric ABO_3-phases vary slightly between the systems, but are generally very close to n:m = 1:2. As can be seen in Fig. 1, it is difficult to obtain very low concentrations of alkali metals, as even the 1:9 pulsing ratio results in 20–30 cation % alkali metal in the films.

This is consistent with earlier reports of lithium ALD-processes and shows that the alkali metal of the precursor diffuses into the film and is not restricted to just surface seats. Attempts to deposit films at a higher alkali metal precursor pulse than the 1:1 ratio resulted in very rough films with appearance almost like deposited powders. Between the 1:1 and 1:9 pulsing ratios one can reproducibly control the composition in the films with an accuracy of about one cation percent. It is interesting to note the similarity of the four systems with respect to the ratio of the precursor pulses. A small difference can be found between the pair of sodium- and potassium processes, being that the potassium concentration at low n:m is higher than in the respective sodium processes. This feature is also reported earlier for sodium- and potassium containing materials grown with atomic layer deposition.[28] This may reflect the structure of the alkali metal precursors, as the potassium *tert*-butoxide is a tetramer in gas phase whereas the sodium *tert*-butoxide is a hexamer.[28]

The growth rate of the end member systems as a function of the ratio between alkali- and group 5 precursor pulses was studied. In Fig. 2, the growth rates are given in Å/binary cycle, showing the growth *per metal pulse*.

Once again, the relative similarity between the four end member systems is observed. However, a clear difference is observed between the sodium- and potassium based processes. The growth rate of the sodium systems flatten out at

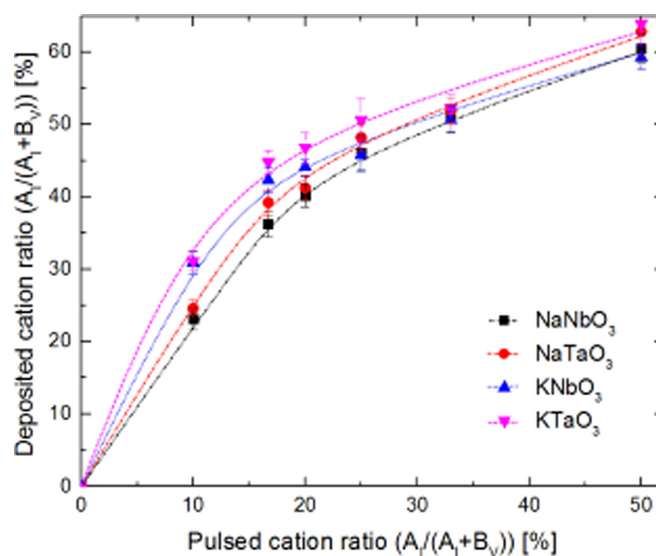

Fig. 1. (Color online) Obtained Na/K:Nb/Ta-ratio in thin films as a function of pulsed cationic ratio. The processes are very similar as the alkali metal content quickly increases even for low pulsed concentration.

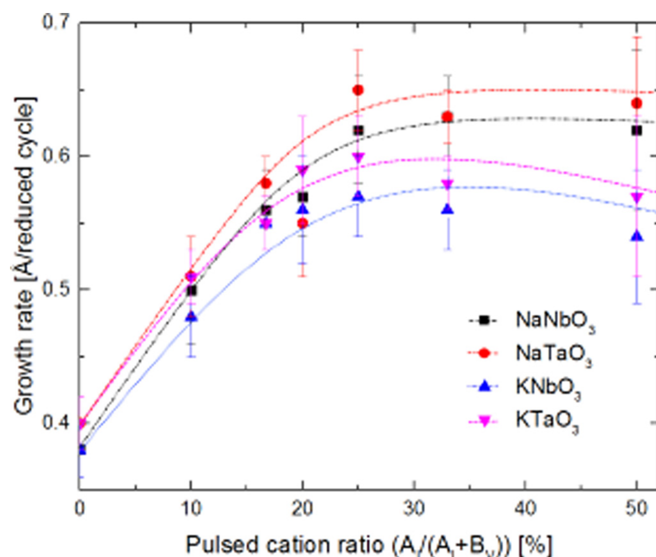

FIG. 2. (Color online) Growth rate of the $A^{I}B^{V}O_3$-systems as a function of pulsed cationic ratio.

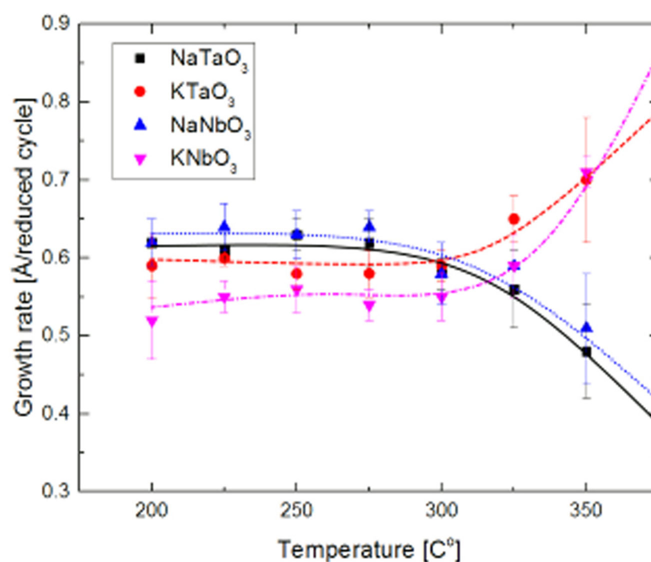

FIG. 3. (Color online) Growth rate of the four $A^{I}B^{V}O_3$-systems as a function of deposition temperature.

around 30% sodium *tert*-butoxide pulses, and are relatively constant for higher ratios. The potassium processes have a maximum growth rate around 25% potassium *tert*-butoxide, but then drops for higher ratios. This is consistent with earlier reports using these precursors.[28] The growth rates for the 1:1 stoichiometric ABO_3 phases are 0.63 ± 0.03, 0.63 ± 0.02, 0.56 ± 0.03, and 0.58 ± 0.02 Å/binary cycle for $NaNbO_3$, $NaTaO_3$, $KNbO_3$, and $KTaO_3$, respectively. With the pulse times used, this corresponds to a growth rate of approximately 0.02 nm/s, yielding a 100 nm film in around 1 h. The uniformity is high for all end member systems, with a gradient of 5%–6% across the deposition chamber (slightly higher growth rate at the inlet). The nonuniformity is less than 1% for a $1 \times 1\ cm^2$ substrate positioned in the middle of the chamber.

The temperature dependence of the growth was studied inside the working range for precursors, from 200 to 350 °C (Fig. 3).

The growth rate of the sodium containing thin films was relatively constant up to approximately 300 °C, whereafter it dropped considerably. A similar stability was seen for the potassium containing thin films, but here the growth rate *increased* rapidly above 300 °C. The potassium films deposited above 300 °C show severe inhomogeniety and have higher carbon contents than films deposited at lower temperatures. This points toward the formation of potassium carbonate at higher temperatures, consistent with earlier reports, including growth rates for sodium- and potassium containing thin films at temperatures above 300 °C.

There are large variations in the composition of the deposited products on increasing temperature (Fig. 4).

Above 300 °C, the sodium content drops while the potassium content increases. This supports the suggestion that the variation in growth rates between Na- and K-systems are due to the nature of the alkali metal precursors. At temperatures below 200 °C, severe nonuniformity in the stoichiometry of the obtained products is observed (not shown), possibly due to a low thermal gradient between the alkali metal precursor hot sources and the reaction chamber. The applicable temperature range for the chosen precursors is between 200 and 300 °C.

The similarity of the growth rates of the end member systems suggests that they may be mixed to form the even more interesting quaternary and possibly quinary phases. A large set of deposition experiments were performed to examine all combinations of quaternary mixes, in addition to a proof of concept deposition for the quinary $K_xNa_{1-x}Nb_yTa_{1-y}O_3$ phase. The results of the quaternary depositions are shown in Fig. 5.

The small difference in growth rates between the Nb- and Ta-, and -K and Na-systems are apparent also in these experiments. The $(K/Na)Nb_xTa_{1-x}O_3$ mixes are slightly tantalum rich, and the $K_xNa_{1-x}(Nb/Ta)O_3$-mixes are slightly potassium rich as compared to targeted 1:1 stoichiometric

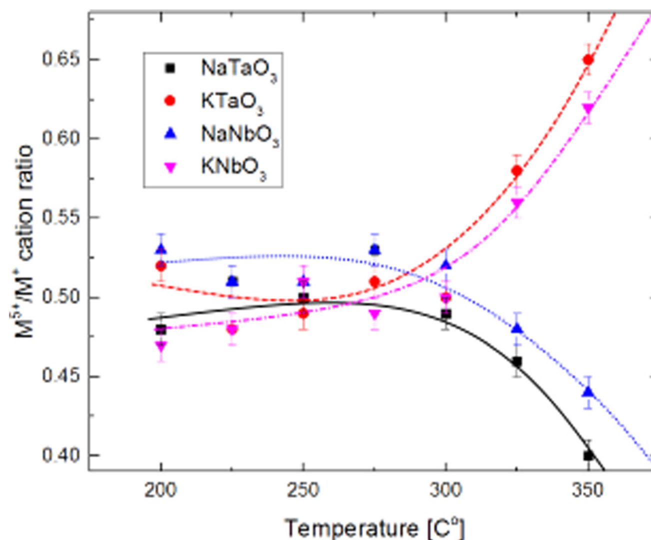

FIG. 4. (Color online) Net cation ratio for the $A^{I}B^{V}O_3$-systems as a function of deposition temperature.

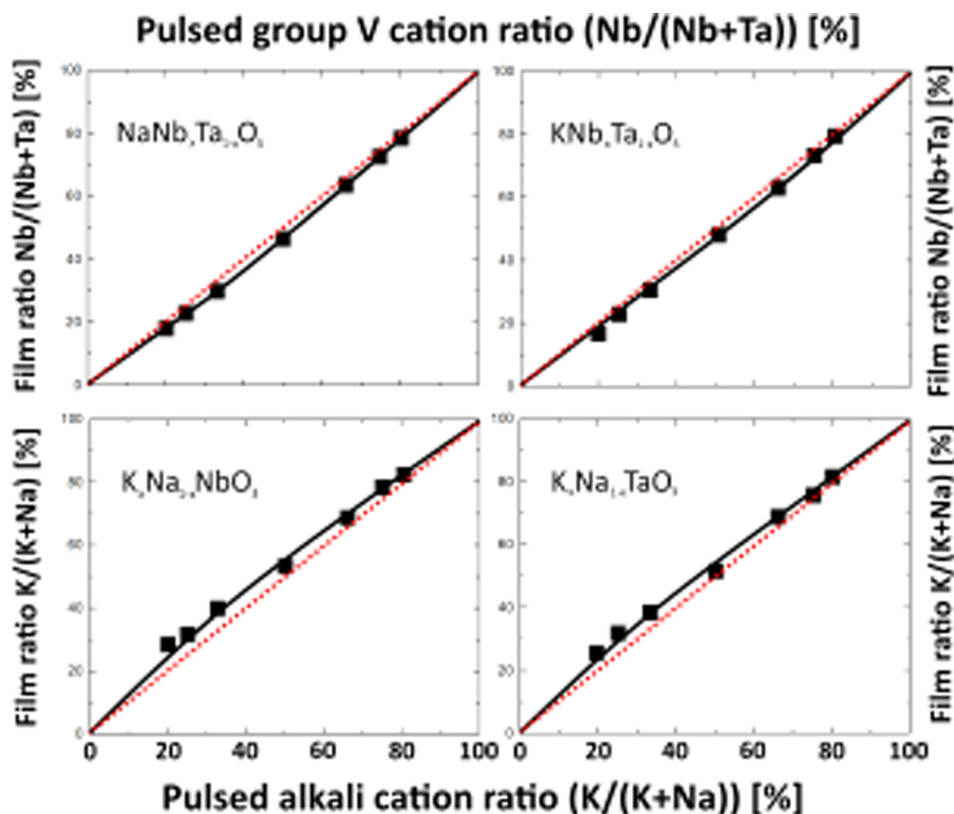

FIG. 5. (Color online) Intermixing on the cation and anion site for the four end member systems to form quaternary compounds. The dotted red line indicates a 1:1 linear intermixing; uncertainties within the size of symbols.

mixing. However, tuning of pulsed ratios is well feasible in order to obtain targeted phases and compositions. For proof of concept, a stoichiometric $K_{0.5}Na_{0.5}NbO_3$ thin film was deposited using a pulsed K:Na ratio of 48:52.

The quinary $K_xNa_{1-x}Nb_yTa_{1-y}O_3$-phase was deposited to fully prove the complete mixing of the involved cation systems, yielding a close to stoichiometric $K_{0.5}Na_{0.5}Nb_{0.5}Ta_{0.5}O_3$ film at K:Na = 48:52 and Nb:Ta = 51:49 pulsing ratios, respectively. It should be noted that these films were heat treated before measuring the composition, facilitating improved cation mixing in the films by thermal diffusion.

B. Morphology and structure

All systems investigated in this study were amorphous as deposited on silicon substrates. This is as expected due to the amorphous nature of the native silicon oxide layer on the silicon substrates. *In situ* annealing GIXRD experiments revealed that all four end-member structures remain x-ray amorphous up to 500 °C, and then turn polycrystalline in a perovskite- or perovskitelike structure. At 750 °C, the long order disappears, and the films become x-ray amorphous again. At 800 °C, any signs of crystallinity completely disappear; see Fig. 6 for $NaNbO_3$.

The latter conversion is irreversible as no long range order reappeared during cooling. Subsequent XPS measurements revealed lower alkali metal content after annealing above the critical temperature for amorphization, pointing toward evaporation of alkali compounds or diffusion of alkali ions into the substrate. This has also been observed in Li-containing atomic layer deposited thin films.[25]

The morphology of the $A^IB^VO_3$ films was analyzed using AFM in a noncontact tapping mode as the as-deposited amorphous films were atomically flat, with a measured mean roughness of 0.1–0.3 nm. After annealing at 500 °C for 10 min, the morphology changed drastically with the formation of small crystallites (Fig. 7).

No apparent order of the crystallites is visible, but there is an observable difference in the morphology of the niobium-

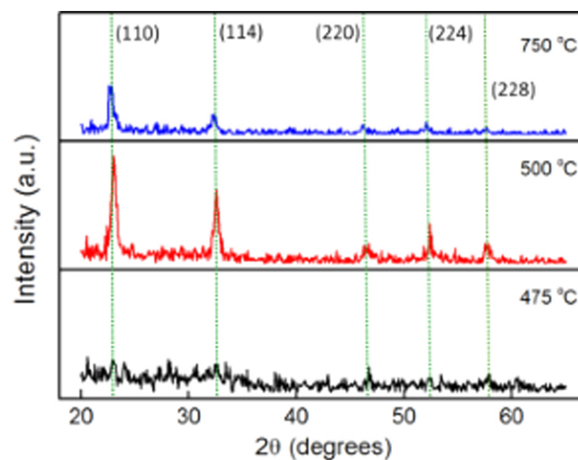

FIG. 6. (Color online) Grazing incidence diffraction patterns showing the temperature evolution of the crystallinity in $NaNbO_3$ thin films as a typical example for crystallization of $A^IB^VO_3$ films.

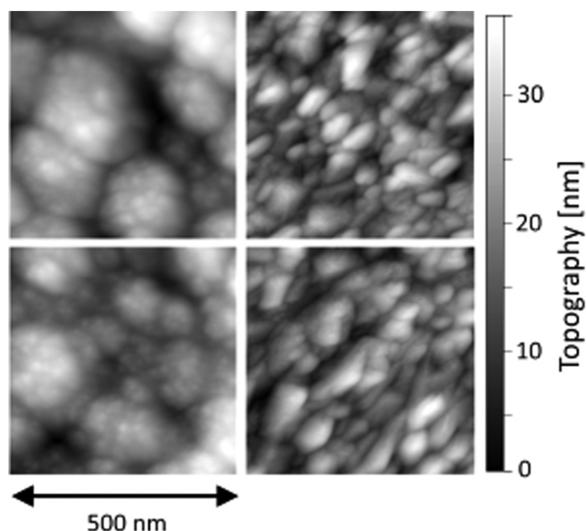

FIG. 7. Morphology of $A^IB^VO_3$ thin films annealed at 500 °C; compositions included in the figures.

and tantalum-based films. The niobium based films exhibit some large crystallites with many very small crystallites in between. The tantalum based films contain many small crystallites with a more narrow size distribution.

The roughness of the films after annealing was 5.9, 6.2, 5.1, and 6.5 nm for $NaNbO_3$, $NaTaO_3$, $KNbO_3$, and $KTaO_3$, respectively. A simple watershed analysis using the Gwyddion 2.43 SPM visualization tool gave the average size of the crystallites. The large crystallites of $NaNbO_3$ were estimated to be 126 ± 5 nm, whereas the small crystallites were estimated to be 13.8 ± 1.2 nm. For $KNbO_3$, the same numbers were 96 ± 13 and 15 ± 3.3 nm, respectively. The average crystallite sizes of the $NaTaO_3$ and $KTaO_3$ were 33 ± 3 and 43 ± 5 nm, respectively.

As a proof of concept on the technological implications of this research, a $K_{0.5}Na_{0.5}NbO_3$ thin film was deposited on a Pt-coated Si-wafer for subsequent electric characterization. The potassium sodium niobate (KNN) thin film exhibits well defined domains with antiparallel piezoelectric response (Fig. 8).

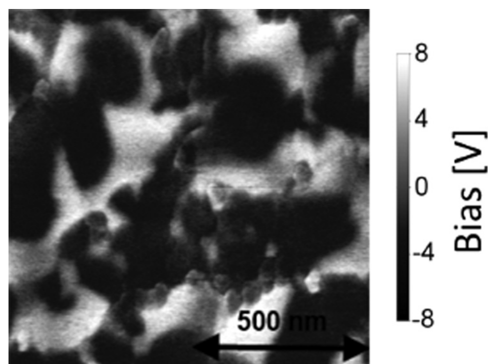

FIG. 8. Enhanced piezoelectric force microscopy on a $K_{0.5}Na_{0.5}NbO_3$ thin film deposited on a Pt-coated silicon substrate and annealed at 500 °C for 10 min. The map shows separated domains with the polar vector normal to the substrate surface. The small grains with 0 V electric response is possibly precipitated Nb_2O_5 due to a slightly overstoichiometry of niobium in the films.

The separate regions are ordered with a 180° phase difference, showing that the polar axis is aligned normal to the substrate. The ALD technique proved further applicable to vary the stoichiometry close to the morphotropic phase boundary and thereby to tune the electric properties.

IV. SUMMARY AND CONCLUSIONS

Atomic layer deposition of the four important perovskites $NaNbO_3$, $NaTaO_3$, $KNbO_3$, and $KTaO_3$ is reported for the first time. These ternary oxides exhibit similar growth behaviors and all can be deposited between 200 and 300 °C. The as deposited films are amorphous on silicon substrates and crystallize during annealing at 500 °C for 10 min. The resulting crystallites are between 80 and 180 nm in size for the niobium based films and between 30 and 50 nm for the tantalum based films, being randomly oriented. Annealing at above 800 °C results in alkali metal loss and irreversible degradation.

Intermixing of the four cations while keeping good control of stoichiometry has been demonstrated. Among the interesting quaternary phases that can be deposited is the technologically important KNN, which was successfully deposited on the Pt-coated silicon substrates and showed antiparallel piezoelectric domains after post-treatment.

ACKNOWLEDGMENTS

The authors would like to acknowledge the Department of Geology at the University of Oslo for the use of and support with XRF instrumentation. They would also like to thank Erik Østreng, Ph.D., for taking part in XRD-studies and fruitful discussion.

[1]B. T. Matthias and J. P. Remeika, Phys. Rev. **76**, 1886 (1949).
[2]S. C. Abrahams, J. M. Reddy, and J. L. Bernstein, J. Phys. Chem. Solids **27**, 997 (1966).
[3]K. Nassau, H. J. Levinstein, and G. M. Loiacono, J. Phys. Chem. Solids **27**, 983 (1966).
[4]L. Egerton and D. M. Dillon, J. Am. Ceram. Soc. **42**, 438 (1959).
[5]N. Yoshifumi, S. Wataru, M. Hiroshi, S. Tetsuo, and Y. Toshinobu, Jpn. J. Appl. Phys. **46**, 311 (2007).
[6]Y. Tomoaki, I. Hiroshi, and N. Nobukazu, Jpn. J. Appl. Phys., Part 1 **8**, 1127 (1969).
[7]H. Kato, K. Asakura, and A. Kudo, J. Am. Chem. Soc. **125**, 3082 (2003).
[8]U. Yutaka, Jpn. J. Appl. Phys., Part 1 **13**, 1362 (1974).
[9]D. Xue and S. Zhang, Chem. Phys. Lett. **291**, 401 (1998).
[10]K. Zou, S. Ismail-Beigi, K. Kisslinger, X. Shen, D. Su, F. J. Walker, and C. H. Ahn, APL Mater. **3**, 036104 (2015).
[11]M. Sepliarsky, S. Phillpot, D. Wolf, M. Stachiotti, and R. Migoni, J. Appl. Phys. **90**, 4509 (2001).
[12]S. Takehisa, A. Harumi, W. Takahiro, and A. Hideaki, Jpn. J. Appl. Phys., Part 1 **44**, 6969 (2005).
[13]S. Kenji, O. Fumihito, N. Akira, M. Tomoyoshi, and K. Isaku, Jpn. J. Appl. Phys., Part 1 **47**, 8909 (2008).
[14]J. Narkilahti and M. Tyunina, J. Phys.: Condens. Matter **24**, 325901 (2012).
[15]C. Zaldo, D. Gill, R. Eason, J. Mendiola, and P. Chandler, Appl. Phys. Lett. **65**, 502 (1994).
[16]S. S. Thöny, H. Lehmann, and P. Günter, Appl. Phys. Lett. **61**, 373 (1992).
[17]S. Takada, M. Ohnishi, H. Hayakawa, and N. Mikoshiba, Appl. Phys. Lett. **24**, 490 (1974).
[18]J.-W. Son, S. S. Orlov, B. Phillips, and L. Hesselink, J. Electroceram. **17**, 591 (2006).

[19]Z. Sitar, F. Gitmans, W. Liu, and P. Günter, MRS Proceedings, 1995 (unpublished).
[20]J. A. Agostinelli, G. H. Braunstein, and T. N. Blanton, Appl. Phys. Lett. **63**, 123 (1993).
[21]Y. Saito and T. Shiosaki, Jpn. J. Appl. Phys., Part 1 **30**, 2204 (1991).
[22]S.-C. Jung and N. Imaishi, Korean J. Chem. Eng. **16**, 229 (1999).
[23]M. V. Romanov, I. E. Korsakov, A. R. Kaul, S. Y. Stefanovich, I. A. Bolshakov, and G. Wahl, Chem. Vap. Deposition **10**, 318 (2004).
[24]M. Kadota and H. Tochishita, IEEJ Trans. Commun. **131**, 1188 (2011).
[25]E. Østreng, H. H. Sønsteby, T. Sajavaara, O. Nilsen, and H. Fjellvåg, J. Mater. Chem. C **1**, 4283 (2013).
[26]J. Liu, M. N. Banis, X. Li, A. Lushington, M. Cai, R. Li, T.-K. Sham, and X. Sun, J. Phys. Chem. C **117**, 20260 (2013).
[27]S. M. George, Chem. Rev. **110**, 111 (2009).
[28]E. Østreng, H. Sønsteby, S. Øien, O. Nilsen, and H. Fjellvåg, Dalton Trans. **43**, 16666 (2014).
[29]K. Kukli, M. Ritala, and M. Leskelä, J. Electrochem. Soc. **142**, 1670 (1995).
[30]K. Kukli, M. Ritala, M. Leskelä, and R. Lappalainen, Chem. Vap. Deposition **4**, 29 (1998).
[31]D. Nečas and P. Klapetek, Open Phys. **10**, 181 (2011).
[32]P. Güthner and K. Dransfeld, Appl. Phys. Lett. **61**, 1137 (1992).
[33]See supplementary material at http://dx.doi.org/10.1116/1.4953406 for information of the self-limiting growth of the niobium and tantalum precursors.